J|A|C|S ARTICLES

Published on Web 06/24/2009

Homoconjugation/Homoaromaticity in Main Group Inorganic Molecules

Qin Zhang,[†] Shiping Yue,[†] Xin Lu,[*,†] Zhongfang Chen,[*,‡] Rongbin Huang,[†] Lansun Zheng,[†] and Paul von Ragué Schleyer[#]

State Key Laboratory for Physical Chemistry of Solid Surface and Center for Theoretical Chemistry, College of Chemistry and Chemical Engineering, Xiamen University, Xiamen 361005, China, Department of Chemistry, Institute for Functional Nanomaterials, University of Puerto Rico, Rio Piedras Campus, San Juan, Puerto Rico 00931, and Department of Chemistry, University of Georgia, Athens, Georgia 30602

Received April 13, 2009; E-mail: xinlu@xmu.edu.cn; zhongfangchen@gmail.com

Abstract: Quantum chemical computations show that three groups of inorganic ions and neutral molecules, whose structures have long been known and characterized, are aromatic due to through-space homoconjugation: (i) I_4^{2+}, $S_6N_4^{2+}$, and $S_2I_4^{2+}$ dications and the $(O_2)_4$ cluster with pericyclic transition-state-like (PTS-like) homoaromaticity; (ii) the bishomoaromatic Te_6^{2+} and 1,5-diphosphadithiatetrazocines; and (iii) the spherically homoaromatic Te_6^{4+}. The $S_2I_4^{2+}$ dication has an unusually high S−S bond order (∼2.3) and dual PTS-like aromaticity arising from two separate sets of four-center, six-electron (4c-6e) in-plane through-space conjugation. The diamagnetic $(O_2)_4$ structural unit recently observed in ε-phase oxygen solid has quadruple PTS-like aromaticity, each arising from 4c-6e in-plane through-space conjugation within an O_2-O_2 plane. Finally, we note that the lighter S_6^{4+} and Se_6^{4+} homologues of Te_6^{4+} also are spherically homoaromatic and might be observable in complexes.

1. Introduction

Johannes Thiele not only originated the concept of adjacent double bond conjugation in 1899, but he also recognized that the through-space interaction (now called homoconjugation) might confer cycloheptatriene (CHT) with benzene-like aromatic properties.[1] Although the energetic stabilization of CHT is weak, its homoaromaticity finally has been established firmly.[2] Much larger, more easily recognizable effects are found in cationic species. Homoconjugation due to through-space homoallylic conjugation of a nonadjacent C=C double bond with a carbocationic center in the cholesteryl−i-cholesteryl rearrangement **1** was discovered by Shoppee in 1946[3] and elucidated by Winstein in 1948.[4] "Homoaromatic" aptly describes compounds like **2** and **3**, where the cyclic conjugation persists uninterrupted despite the presence of one or more saturated linkages.[5,6] As in the well-established continuum of through-bond conjugation in conventional aromatic compounds (e.g., benzene), homoconjugated systems are described as homoaromatic when the number of cyclically delocalized valence electrons fulfills appropriate electron-counting rules, such as the $(4N+2)$ Hückel rule ($N = 0, 1,...$) originally proposed for monocyclic aromatics,[7] the $4N$ rule originally proposed for Möbius-type aromatics,[8] and the $2(N+1)^2$ rule ($N = 0, 1,...$) originally proposed for highly symmetric cage (three-dimensional) systems of spherical aromaticity.[9] Accordingly, the aromaticity arising from *homoconjugation* can be roughly classified as Hückel-type homoaromaticity (e.g., as in cations **2** and **3** and the cycloaddition transition state **4**),[5,6] Möbius-type homoaromaticity[8,10,11] (e.g., as in the electrocyclic reaction transition states **5** and **6**), and spherical homoaromaticity (e.g., as in 1,3-dehydro-5,7-admantanediyl dication **7**),[9,12] depending on the geometry of the homoconjugative system and the number of delocalized electrons involved.

[†] Xiamen University.
[‡] University of Puerto Rico.
[#] University of Georgia.

(1) Thiele, J. *Annalen* **1899**, *306*, 87.
(2) Chen, Z.; Jiao, J.; Wu, J. I.; Herges, R.; Zhang, S. B.; Schleyer, P. v. R. *J. Phys. Chem. A* **2008**, *112*, 10586.
(3) Shoppee, C. W. *J. Chem. Soc.* **1946**, 1147.
(4) (a) Winstein, S.; Adams, R. *J. Am. Chem. Soc.* **1948**, *70*, 838. (b) Simonetta, M.; Winstein, S. *J. Am. Chem. Soc.* **1954**, *76*, 18.
(5) (a) Winstein, S. *J. Am. Chem. Soc.* **1959**, *81*, 6524. (b) Winstein, S.; Sonnenberg, J.; deVeries, L. *J. Am. Chem. Soc.* **1959**, *81*, 6523.
(6) (a) Winstein, S. *Chem. Soc. Spec. Publ.* **1967**, *21*, 5. (b) Paquette, L. A. *Angew. Chem., Int. Ed. Engl.* **1978**, *17*, 106. (c) Childs, R. F. *Acc. Chem. Res.* **1984**, *17*, 347. (d) Williams, R. V.; Kurtz, H. A. *Adv. Phys. Org. Chem.* **1994**, *29*, 273. For recent reviews on homoaromaticity, see: (e) Williams, R. V. *Chem. Rev.* **2001**, *101*, 1185. (f) Williams, R. V. *Eur. J. Org. Chem.* **2001**, 227.
(7) Hückel, E. *Z. Phys.* **1931**, *70*, 204.
(8) (a) Heilbronner, E. *Tetrahedron Lett.* **1964**, 1923. (b) Rzepa, H. S. *Chem. Rev* **2005**, *105*, 3697, and references therein.
(9) (a) For the spherical aromaticity of fullerenes, see: Hirsch, A.; Chen, Z.; Jiao, H. *Angew. Chem., Int. Ed.* **2000**, *39*, 3915. For reviews on spherical aromaticity, see: (b) Bühl, M.; Hirsch, A. *Chem. Rev.* **2001**, *101*, 1153. (c) Chen, Z.; King, R. B. *Chem. Re.v* **2005**, *105*, 3613. Spherical homoaromaticity was also reviewed in the latter.
(10) For a recent review on the applications of nucleus-independent chemical shift, see: Chen, Z.; Wannere, C. S.; Corminboeuf, C.; Puchta, R.; Schleyer, P. v. R. *Chem. Rev.* **2005**, *105*, 3842 Pericyclic-reaction transition states with Hückel- or Möbius-type homoaromaticity were reviewed therein.
(11) (a) Rzepa, H. S. *Org. Lett.* **2008**, *10*, 949. (b) Rappaport, S. M.; Rzepa, H. S. *J. Am. Chem. Soc.* **2008**, *130*, 7613. (c) Allan, C. S. M.; Rzepa, H. S. *J. Chem. Theory Comput.* **2008**, *4*, 1841. (d) Allan, C. S. M.; Rzepa, H. S. *J. Org. Chem.* **2008**, *73*, 6615.
(12) Chen, Z.; Jiao, H. J.; Hirsch, A.; Schleyer, P. v. R. *Angew. Chem., Int. Ed.* **2002**, *41*, 4309.

Scheme 1. Representative Organic Systems with Homoconjugation-Induced Homoaromaticity

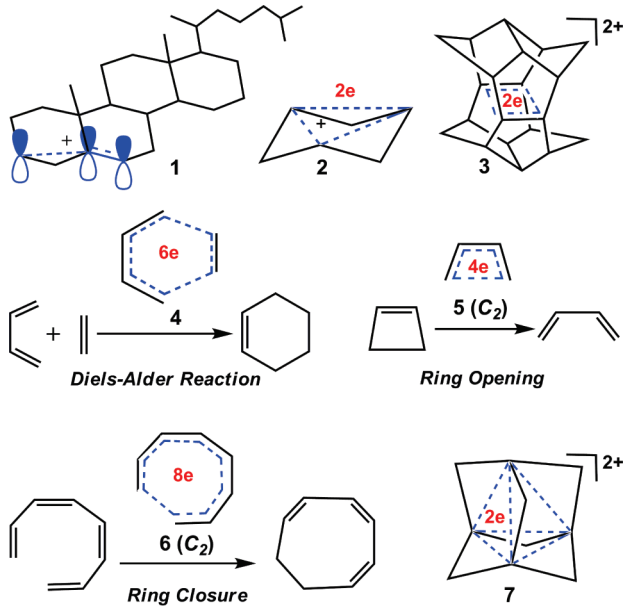

Homoconjugation as well as homoaromaticity has been widely recognized in a large number of organic compounds and ions (Scheme 1). More specifically, a Hückel-type homoaromatic compound has one or more saturated linkages to interrupt the formal cyclic delocalization of $4N+2$ π-electrons. For example, the dication **2** with "monocyclic" three-center, two-electron (3c-2e) homoconjugation interrupted by three saturated $>CH_2$ groups is *trishomoaromatic*; the pagodane dication **3** is *bishomoaromatic* due to "monocyclic" four-center, two-electron (4c-2e) homoconjugation with two saturated linkages (Scheme 1). A large number of organic cationic and anionic systems have been demonstrated to show such Hückel-type homoaromaticity from theoretical and experimental investigations.[6,13] Hückel-type homoconjugation can also be found within the transition states of some organic pericyclic reactions (e.g., the Diels−Alder reactions and Cope rearrangements) that involve a total of $4N+2$ ($N = 0, 1, 2,...$) conjugative electrons, namely, aromaticity of pericyclic transition states (PTS),[14,15] despite the absence of saturated linkages between the spaced homoconjugative subunits. For instance, the transition state **4** of the prototype Diels−Alder reaction, butadiene + ethylene, is aromatic due to homoconjugation of *six mobile electrons* (Scheme 1). On the other hand, transition states of some pericyclic reactions involving $4N$ ($N = 0, 1, 2,...$) homoconjugative electrons can attain Möbius-type homoaromaticity.[10] For instance, the C_2-symmetric transition state **5** for the ring-opening of cyclobutene to butadiene has "monocyclic" four-center, four-electron (4c-4e) through-space conjugation that affords Möbius-type homoaromaticity.[10] Likewise, the C_2-symmetric transition state **6** for the ring-closure of octatetraene is Möbius-homoaromatic. Spherical homoaromaticity can be found within highly symmetrical organic cage molecules (or ions), in which through-space conjugation involves $2(N+1)^2$ electrons.[12] This is exemplified by the 1,3-dehydro-5,7-adamantanediyl dication **7** ($C_{10}H_{12}^{2+}$)[16] with 4c-2e spherical homoaromaticity, in which the four homoconjugative sp^2-hybridized carbon atoms in the highly symmetrical organic framework are separated by sp^3-hybridized carbon atoms.

Scheme 2. Resonance of Three Valence-Bond Structures To Account for the 6c-10e Through-Space π-Homoconjugation within $Se_2I_4^{2+}$

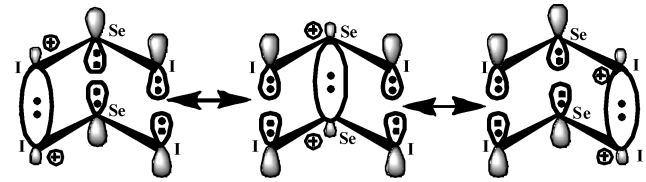

Although through-space homoconjugation is well established in organic chemistry,[17] its role in inorganic ions and compounds is much less clearly recognized. Is similar aromatic through-space homoconjugation present in inorganic systems? Our preliminary work showed that the inorganic $Se_2I_4^{2+}$ and $S_2O_4^{2-}$ ions possess aromatic through-space six-center, ten-electron (6c-10e) conjugation (Scheme 2).[18] Since the effects are analogous to the through-space homoconjugation in the pericyclic transition states of Diels−Alder reactions and Cope rearrangements, the aromaticity in $Se_2I_4^{2+}$ and $S_2O_4^{2-}$ was termed as pericyclic transition-state-like aromaticity (PTS-like aromaticity). We now show, by means of quantum chemical calculations, that aromatic through-space homoconjugations do exist in several well-characterized inorganic compounds and ions and can be classified into three groups: (i) PTS-like homoaromaticity in I_4^{2+},[19] $S_6N_4^{2+}$,[20] $S_2I_4^{2+}$,[21] and the diamagnetic $(O_2)_4$ unit in

(13) (a) Prakash, G. K.; Krishnamurthy, V. V.; Herges, R.; Bau, R.; Yuan, H.; Olah, G. A.; Fessner, W. D.; Prinzbach, H. *J. Am. Chem. Soc.* **1986**, *108*, 836. (b) Prakash, G. K.; Surya, K., V. V.; Herges, R.; Bau, R.; Yuan, H.; Olah, G. A.; Fessner, W. D.; Prinzbach, H. *J. Am. Chem. Soc.* **1988**, *110*, 7764. (c) Herges, R.; Schleyer, P. v. R.; Schindler, M.; Fessner, W. D. *J. Am. Chem. Soc.* **1991**, *113*, 3649. (d) Etzkorn, M.; Wahl, F.; Keller, M.; Prinzbach, H.; Barbosa, F.; Peron, V.; Gescheidt, G.; Heinze, J.; Herges, R. *J. Org. Chem.* **1998**, *63*, 6080. (e) Surya Prakash, G. K.; Weber, K.; Olah, G. A.; Prinzbach, H.; Wollenweber, M.; Etzkorn, M.; Voss, T.; Herges, R. *Chem. Comm.* **1999**, 1029.
(14) For the pioneering work on transition-state aromaticity, see: (a) Evans, M. G.; Warhurst, E. *Trans. Faraday Soc.* **1938**, *34*, 614. (b) Zimmerman, H. E. *Acc. Chem. Res.* **1971**, *4*, 272. (c) Dewar, M. J. S. *Angew. Chem., Int. Ed.* **1971**, *10*, 761. (d) Cossio, F. P.; Morao, I.; Jiao, H.; Schleyer, P. v. R. *J. Am. Chem. Soc.* **1999**, *121*, 6737.
(15) Wannere, C. S.; Bansal, R. K.; Schleyer, P. v. R. *J. Org. Chem.* **2002**, *67*, 9162.
(16) Bremer, M.; Schleyer, P. v. R.; Schoetz, K.; Kausch, M.; Schindler, M. *Angew. Chem., Int. Ed. Engl.* **1987**, *26*, 761.
(17) Note that inorganic silicon and germanium analogues of the spherical homoaromatic $C_{10}H_{12}^{2+}$ have been theoretically predicted but not yet synthesized. See: Chen, Z.; Hirsch, A.; Nagase, S.; Thiel, W.; Schleyer, P. v. R. *J. Am. Chem. Soc.* **2003**, *125*, 15507.
(18) Zhang, Q.; Lu, X.; Huang, R. B.; Zheng, L. S. *Inorg. Chem.* **2006**, *45*, 2457.
(19) (a) Gillespie, R. J.; Kapoor, R.; Faggiani, R.; Lock, C. J. L.; Murchie, M. P.; Passmore, J. *J. Chem. Soc., Chem. Commun.* **1983**, 8. (b) Faggiani, R. J.; Gillespie, R. J.; Kapoor, R.; Lock, C. J. L.; Vekris, J. E. *Inorg. Chem.* **1988**, *27*, 4350.
(20) (a) Banister, A. J.; Clarke, H. G.; Tayment, I.; Shearer, H. M. M. *Inorg. Nucl. Chem. Lett.* **1974**, *10*, 647. (b) Krebs, B.; Henkel, G.; Pohl, S.; Roesky, H. W. *Chem. Ber.* **1980**, *113*, 226.
(21) (a) Brownridge, S.; Cameron, T. S.; Du, H.; Knapp, C.; Köppe, R.; Passmore, J.; Rautiainen, J. M.; Schnöckel, H. *Inorg. Chem.* **2005**, *44*, 1660, and references therein. (b) Brownridge, S.; Crawford, M.-J.; Du, H.; Harcourt, R. D.; Knapp, C.; Laitinen, R. S.; Passmore, J.; Rautiainen, J. M.; Suontamo, R. T.; Valkonen, J. *Inorg. Chem.* **2007**, *46*, 681.
(22) For the first synthesis of ε-O_2 solid, see: (a) Nicol, M.; Hirsch, K. R.; Holzapfel, W. B. *Chem. Phys. Lett.* **1979**, *68*, 49. For X-ray investigations of ε-O_2 solid, see: (b) Lundegaard, L. F.; Weck, G.; McMahon, M. I.; Desgreniers, S.; Loubeyre, P. *Nature* **2006**, *443*, 201. (c) Fujihisa, H.; Akahama, Y.; Kawamura, H.; Ohishi, Y.; Shimomura, O.; Yamawaki, H.; Sakashita, M.; Gotoh, Y.; Takeya, S.; Honda, K. *Phys. Rev. Lett.* **2006**, *97*, 085503.

ε-phase oxygen solid;[22] (ii) bishomoaromaticity in Te_6^{2+} [23] and 1,5-diphosphadithiatetrazocines $PR_2(NSN)_2PR_2$ (R = methyl, phenyl, Cl);[24] and (iii) spherical homoaromaticity in Te_6^{4+}.[25] More interestingly, the $S_2I_4^{2+}$ ion has dual PTS-like aromaticity arising from two separate through-space four-center, six-electron (4c-6e) homoconjugation sets, which account for the unusually high S−S bond order of 2.2−2.4, suggested by experiments. Moreover, the diamagnetic $(O_2)_4$ unit in solid ε-phase oxygen has quadruple PTS-like aromaticity arising from four separate through-space 4c-6e homoconjugation sets.

2. Computational Details

Geometries were fully optimized, and vibrational frequencies were computed to characterize the nature of the stationary points. For the I_4^{2+}, $S_2I_4^{2+}$, Te_6^{2+}, and X_6^{4+} (X = Te, Se, and S) cations containing third- and fourth-period elements, the hybrid MPW1PW91 density functional[26,27] was employed with the relativistic effective core potentials (RECP)[28a] plus valence triple-ζ basis set (denoted SDB-cc-pVTZ) for I, Te, and Se[28b] and the standard all-electron split-valence 6-311+G(3df) basis set for S. This level of theory reproduces the geometries and properties of chalcogen ions such as S_8^{2+} and Se_8^{2+} with reasonable accuracy.[29] The B3LYP/6-311+G(3df) density functional level,[30,31] previously employed to compute SN-containing species (e.g., S_3N_3),[32] was used for $S_6N_4^{2+}$, for 1,5-diphoshadithiazocines, $PRR'(NSN)_2PRR'$ (R = R′ = CH_3 or R = Cl, R′ = CCl_3), and for $(O_2)_4$. The B3LYP computations on 1,5-diphoshadithiazocine $P(C_6H_5)_2(NSN)_2P(C_6H_5)_2$ were carried out with the 6-311+G(3df) basis set for P, N, and S and the smaller 6-31G(d) basis set for C and H in the phenyl groups.

Computed nucleus-independent chemical shifts (NICS)[10,33,34] at geometric centers, using the same theoretical level as the geometry optimizations, characterized the aromaticity of the inorganic compounds and ions. Significantly negative (diatropic) NICS values indicate aromaticity, whereas appreciably positive (paratropic) NICS values are associated with antiaromaticity. Refined (CMO-NICS)[35] computations gave the individual canonical molecular orbital (MO) contributions to the total NICS value for the representative I_4^{2+}, $S_6N_4^{2+}$, and Te_6^{4+} systems at the GIAO-PW91PW91−natural bond orbitals (NBO) level of theory.[36] The NICS out-of-plane *zz* tensor component, a superior NICS index for planar π systems,[37] was examined for I_4^{2+} and $S_6N_4^{2+}$.

The exaltation of diamagnetic susceptibility (MSE), first introduced by Pascal in 1910, is another magnetic criterion of aromaticity indicating the presence of cyclic delocalization of electrons.[38] Dauben et al. surveyed the MSEs of aromatic hydrocarbons systematically in 1968.[39] Subsequent applications of this magnetic aromaticity criterion have characterized, e.g., the homo- and bishomoaromaticity in the homo- and bishomotropenylium as well as the barbaralyl cation,[40] the aromaticity of pericyclic transition states,[41] the double aromaticity of the 3,5-dehydrophenyl cation,[42] and various organic compounds.[43] The MSE (Λ), defined as $\Lambda = \chi_M - \chi_M'$, is the difference between the measured magnetic susceptibility (χ_M) of the aromatic molecule and the susceptibility (χ_M') of a nonaromatic reference system or a value based on an increment scheme.[42] We computed magnetic susceptibilities (χ) with the continuous set of gauge transformations (CSGT)[44] as implemented in the Gaussian 98 program.[45]

3. Results and Discussion

3.1. PTS-like Aromatic Inorganic Ions: I_4^{2+} and $S_6N_4^{2+}$. The dication I_4^{2+} **8** moiety in its salts is disclosed by X-ray crystallography to have a planar rectangular geometry consisting of two I_2^+ monomers.[19] Our MPW1PW91 computations find

(23) (a) Prince, D. J.; Corbett, J. D.; Garbisch, B. *Inorg. Chem.* **1970**, *9*, 2731. (b) Beck, J.; Bock, G. *Z. Naturforsch. B* **1996**, *51*, 119. (c) Beck, J.; Bock, G. *Z. Anorg. Allg. Chem.* **1996**, *622*, 823. (d) Beck, J. *Chem. Ber.* **1995**, *128*, 23.

(24) (a) Burford, N.; Chivers, T.; Codding, P. W.; Oakley, R. T. *Inorg. Chem.* **1982**, *21*, 982. (b) Chivers, T.; Edwords, M.; Parvez, M. *Inorg. Chem.* **1992**, *31*, 1861.

(25) Burns, R. C.; Gillespie, R. J.; Luk, W. C.; Slim, D. R. *Inorg. Chem.* **1979**, *18*, 3086.

(26) (a) Adamo, C.; Barone, V. *Chem. Phys. Lett.* **1997**, *274*, 242. (b) Adamo, C.; Barone, V. *J. Chem. Phys.* **1998**, *108*, 664.

(27) Perdew, J. P.; Wang, Y. *Phys. Rev.* **1992**, *B45*, 13244.

(28) (a) Bergner, A.; Dolg, M.; Kuechle, W.; Stoll, H.; Preuss, H. *Mol. Phys.* **1993**, *80*, 1431. (b) Martin, J. M. L.; Sundermann, A *J. Chem. Phys.* **2001**, *114*, 3408. The 46-, 28-, and 46-electron core pseudopotentials have been used for I, Se, and Te, respectively. The SDB-cc-pVTZ basis sets and the related pseudopotentials are available at the EMSL basis set library (https://bse.pnl.gov/bse/portal). For details of this library, see: (c) Feller, D. *J. Comput. Chem.* **1996**, *17*, 1571. (d) Schuchardt, K. L.; Didier, B. T.; Elsethagen, T.; Sun, L.; Gurumoorthi, V.; Chase, J.; Li, J.; Windus, T. L. *J. Chem. Inf. Model.* **2007**, *47*, 1045.

(29) Gameron, T. S.; Deeth, R. J.; Dionne, I.; Du, H. B.; Jenkins, H. D. B.; Krossing, I.; Passmore, J.; Roobottom, H. K. *Inorg. Chem.* **2000**, *39*, 5614.

(30) (a) Becke, A. D. *J. Chem. Phys.* **1993**, *98*, 5648. (b) Lee, C.; Yang, W.; Parr, R. G. *Phys. Rev. A* **1988**, *37*, 785.

(31) Glukhovtsev, M. N.; Pross, A.; McGrath, M. P.; Radom, L. *J. Chem. Phys.* **1995**, *103*, 1878.

(32) (a) Messerschmidt, M.; Wagner, A.; Wong, M. W.; Luger, P *J. Am. Chem. Soc.* **2002**, *124*, 732. (b) Proft, F. D.; Fowler, P. W; Havenith, R. W. A.; Schleyer, P. v. R.; Lier, G. V.; Geerlings, P. *Chem.—Eur. J.* **2004**, *10*, 940.

(33) (a) Schleyer, P. v. R.; Maerker, C.; Dransfeld, A.; Jiao, H. J.; Hommes, N. J. R. v. E. *J. Am. Chem. Soc.* **1996**, *118*, 6317. (b) Schleyer, P. v. R.; Jiao, H.; Hommes, N. J. R. v. E.; Malkin, V. G.; Malkina, O. L. *J. Am. Chem. Soc.* **1997**, *119*, 12669.

(34) Wolinski, K.; Hilton, J. F.; Pulay, P. J. *J. Am. Chem. Soc.* **1990**, *112*, 8251, and references therein.

(35) Heine, T.; Schleyer, P. v. R.; Corminboeuf, C.; Seifert, G.; Reviakine, R.; Weber, J. *J. Phys. Chem. A* **2003**, *107*, 6470. (b) Corminboeuf, C.; Heine, T.; Weber, J. *Phys. Chem. Chem. Phys.* **2003**, *5*, 246. (c) Corminboeuf, C.; Heine, T.; Seifert, G.; Schleyer, P. v. R.; Weber, J. *Phys. Chem. Chem. Phys.* **2004**, *6*, 273.

(36) (a) Bohmann, J. A.; Weinhold, F.; Farrar, T. C. *J. Chem. Phys.* **1997**, *107*, 1173–1184. (b) Glendening, E. D.; Badenhoop, J. K.; Reed, A. E.; Carpenter, J. E.; Bohmann, J. A.; Morales, C. M.; Weinhold, F. *NBO 5.0*; Theoretical Chemistry Institute, University of Wisconsin: Madison, WI, 2001; www.chem.wisc.edu/~nbo5.

(37) Fallah-Bagher-Shaidaei, H.; Wannere, C. S.; Corminboeuf, C.; Puchta, R.; Schleyer, P. v. R. *Org. Lett.* **2006**, *8*, 863.

(38) For pioneering work on the exaltation of magnetic susceptibility of aromatic systems, see: (a) Pascal, P. *Ann. Chim. Phys.* **1910**, *19*, 5. (b) Pacault, A. *Ann. Chim., Ser. XII* **1946**, *1*, 567. (c) Pink, R. C. *Trans. Faraday Soc.* **1948**, *4*, 407.

(39) For pioneering work on applications of MSE, see: (a) Dauben, H. P., Jr.; Wilson, J. D.; Laity, J. L. *J. Am. Chem. Soc.* **1968**, *90*, 811. (b) Dauben, H. P., Jr.; Wilson, J. D.; Laity, J. L. *J. Am. Chem. Soc.* **1969**, *91*, 1991. (c) Dauben, H. J., Jr.; Wilson, J. D.; Laity, J. L. In *Nonbenzoid Aromaticity*; Synder, J. P., Ed.; Academic Press: New York, 1971; Vol. 11.

(40) (a) Cremer, D.; Reichel, F.; Kraka, E. *J. Am. Chem. Soc.* **1991**, *113*, 9459. (b) Cremer, D.; Svensson, P.; Kraka, E.; Ahlberg, P. *J. Am. Chem. Soc.* **1993**, *115*, 7445. (c) Cremer, D.; Svensson, P.; Kraka, E.; Konkoli, Z.; Ahlberg, P. *J. Am. Chem. Soc.* **1993**, *115*, 7457.

(41) (a) Jiao, H.; Schleyer, P. v. R. *Angew. Chem., Int. Ed. Engl.* **1993**, *32*, 1763. (b) Jiao, H.; Schleyer, P. v. R. *J. Chem. Soc., Perkin Trans. 2* **1994**, 407. (c) Jiao, H.; Schleyer, P. v. R. *J. Chem. Soc., Faraday Trans.* **1994**, *90*, 1559. (d) Herges, R.; Jiao, H.; Schleyer, P. v. R. *Angew. Chem., Int. Ed. Engl.* **1994**, *33*, 1376.

(42) Schleyer, P. v. R.; Jiao, H.; Glukhovtsev, M. N.; Chandrasekhar, J.; Kraka, E. *J. Am. Chem. Soc.* **1994**, *116*, 10129.

(43) Schleyer, P. v. R.; Jiao, H. *Pure Appl. Chem.* **1996**, *68*, 209.

(44) (a) Keith, T. A.; Bader, R. F. W. *Chem. Phys. Lett.* **1992**, *194*, 1. (b) Keith, T. A.; Bader, R. F. W. *Chem. Phys. Lett.* **1993**, *210*, 223. (c) Cheeseman, J. R.; Frisch, M. J.; Trucks, G. W.; Keith, T. A. *J. Chem. Phys.* **1995**, *104*, 5497.

(45) (a) Frisc; h, M. J.; et al. *Gaussian 98*; Gaussian, Inc.: Pittsburgh, PA, 1998. Electron density plots of selected molecular orbitals were obtained with MOLDEN or MOLEKEL: (b) Schaftenaar, G.; Noordik, J. H. *J. Comput.-Aided Mol. Design* **2000**, *14*, 123. (c) Flükiger, P.; Lüthi, H. P.; Portmann, S.; Weber, J. *MOLEKEL*; CSCS, Swiss National Supercomputing Centre: Manno, Switzerland, 2000.

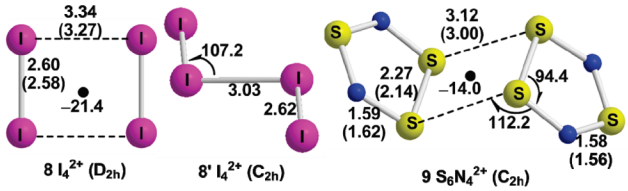

Figure 1. Optimized geometries (bond lengths in Å, angles in degree) and NICS(0) values (in ppm) of I_4^{2+} (**8** and **8′**) and $S_4N_6^{2+}$ **9**, along with the available experimental data (given in parentheses). The theoretical inter-monomer distances are generally within 0.1 Å of the experimental values.

Scheme 3. Four-Center, Six-Electron Through-Space In-Plane π-Conjugation within I_4^{2+}: (a) Molecular Orbital Description and (b) Valence Bond Description

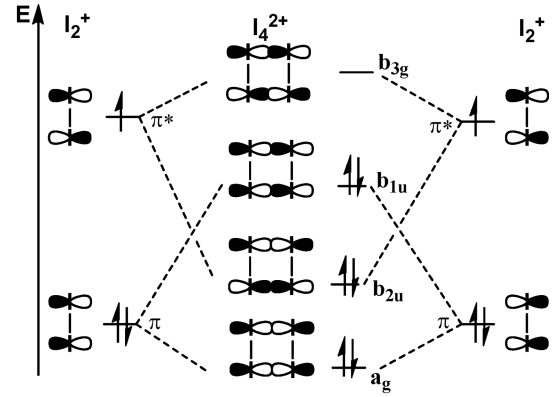

I_4^{2+} **8** to be diamagnetic with a (^1A_g) singlet ground state; its diamagnetic susceptibility, −102.9 ppm·cgs, is in line with measurements.[46] The optimized I−I bond length (∼2.60 Å) of the I_2^+ moieties of I_4^{2+} **8** (Figure 1) is somewhat shorter than the ∼2.67 Å single bond in I_2, implying some intramonomer π-bonding. The intermonomer distance, 3.27 Å, much shorter than the sum of the van de Waals radii (∼4.3 Å), suggests substantial intermonomer interactions. This unusual structural feature has been attributed to the in-plane $\pi^*-\pi^*$ bonding between the two singly occupied π^* orbitals of the I_2^+ monomers (Scheme 3a).[47] Selected MOs of I_4^{2+} **8** (Figure 2a) from our MPW1PW91 calculations confirmed this classic description, in which HOMO−3 is the in-plane $\pi^*-\pi^*$ bonding MO.

The valence bond (VB) description in Scheme 3b also clarifies the intermonomer interaction in I_4^{2+} **8**. The rectangular ground-state geometry results from the resonance of two equivalent VB structures, each having one intermonomer I−I single bond. Such VB resonance, describing through-space in-plane π-conjugation, involves a total of six in-plane p_π-electrons. As this satisfies the (*4N*+2) Hückel rule, the 4c-6e through-space in-plane "π"-conjugation in I_4^{2+} **8** is aromatic.

This characterization is supported by CMO-NICS analysis (Figure 2a and Figure S1 in the Supporting Information). In addition to the six $\pi_{\text{in-plane}}$ electrons, I_4^{2+} (**8**) has eight $\pi_\perp$ electrons. However, the latter contribute very little to the dia-/paratropic character of the whole molecule ((NICS$(\pi_\perp)_{zz}$ = 1.7 ppm) according to CMO-NICS out-of-plane zz tensor analysis. In contrast, the highly diatropic contribution of the six in-plane π electrons (NICS$(\pi_{\text{in-plane}})_{zz}$ = −18.2 ppm) largely determines the total NICS$_{zz}$ value of −23.2 ppm. Since no conventional chemical bond exists between the two I_2^+ species, we describe the 4c-6e through-space conjugation as "PTS-like aromaticity", analogous to the aromatic through-space conjugation discussed previously for the Diels−Alder transition state **4**[10] and the inorganic ions $Se_2I_4^{2+}$ and $S_2O_4^{2-}$.[18]

The cyclic tetragonal I_4^{2+} **8**, featuring through-space in-plane conjugation, is 2.4 kcal/mol lower in energy than its acyclic C_{2h}-symmetric isomer **8′** (Figure 1) at MPW1PW91/SDB-cc-pVTZ, despite the shorter (3.03 Å) intermonomer I···I distance of the latter; **8′** can be regarded as a nonaromatic isomer of **8**. Due to the in-plane homoconjugation, the absolute diamagnetic susceptibility (χ = −102.9 ppm·cgs) computed for the aromatic **8** is much higher than that of the nonaromatic isomer **8′** (χ = −68.2 ppm·cgs); hence, MSE of **8** is −34.7 ppm·cgs.

In addition to I_4^{2+} **8** and **8′**, we have also obtained a D_{4h}-symmetric structure of I_4^{2+}, **8″**, with a I−I distance of 2.92 Å at the same level of theory. This species is aromatic, with a NICS(0) value of −21.1 ppm. However, detailed vibrational analysis indicates this structure is a second-order saddle point 3.27 eV less stable than the D_{2h} structure **8** and corresponds to the concerted transformation of two equivalent C_{2v}-symmetric (I_3^+ + I^+) complexes (see Figure S2 in the Supporting Information for details).

Similar 4c-6e through-space in-plane π-conjugation can be found within the more complex dication $(S_3N_2)_2^{2+}$ **9** (Figure 1), consisting of two $S_3N_2^+$ radicals with 3.0 Å (experimental) intermonomer S···S distances.[20] The radical monomer $S_3N_2^+$ has a singly occupied π^*-orbital and a doubly occupied π-orbital mainly localized around the S−S subunit. Hence, the intermonomer bonding in **9** (Figure 2b) is similar to that of I_4^{2+} (Scheme 3a); note the intermonomer $\pi^*-\pi^*$ bonding orbital (i.e., the HOMO depicted in Figure 2b). Likewise, the VB description depicted in Scheme 3b for I_4^{2+} also can account for the intermonomer 4c-6e through-space in-plane π-conjugation within **9**. The PTS-like aromaticity arising from such intermonomer homoconjugation within **9** is confirmed by our computations, which find a singlet (diamagnetic) ground state and a dominant diatropic contribution of the six in-plane π-electrons (NICS$(\pi_{\text{in-plane}})_{zz}$ = −16.6 ppm) to the total NICS value (NICS(total)$_{zz}$ = −16.0 ppm).

Furthermore, the intermonomer through-space homoconjugation also appears to enhance the π-conjugation in both $S_3N_2^+$ rings of **9**. The NICS(0) value at each $S_3N_2^+$ ring center in **9**, −24.0 ppm (aromatic), is somewhat larger than the −22.6 ppm NICS(0) computed for a single $S_3N_2^{2+}$ dication. The latter has six π-electrons and exhibits typical Hückel-type π-aromaticity.[48] In contrast, the NICS(0) for an individual $S_3N_2^+$ radical is −12.0 ppm at the GIAO-B3LYP/6-311+G(3df) level of theory.

3.2. $S_2I_4^{2+}$: Dual PTS-like Aromaticity. The $S_2I_4^{2+}$ dication **10** in the $S_2I_4(MF_6)_2$ (M = As, Sb) salts was recently reported to have an unusually short S−S bond (1.84 vs ∼2.05 Å for a

(46) Gillespie, R. J.; Morton, M. J.; Milne, J. B. *Inorg. Chem.* **1968**, *7*, 2221.
(47) Brownridge, S.; Krossing, I.; Passmore, J.; Jenkins, H. D. B.; Roobottom, H. K. *Coord. Chem. Rev.* **2000**, *197*, 397.
(48) Zhang, G.; Zhao, Z.; Wu, J. I.; Schleyer, P. v. R. *Inorg. Chem.*, **2009**, *48*, in press.

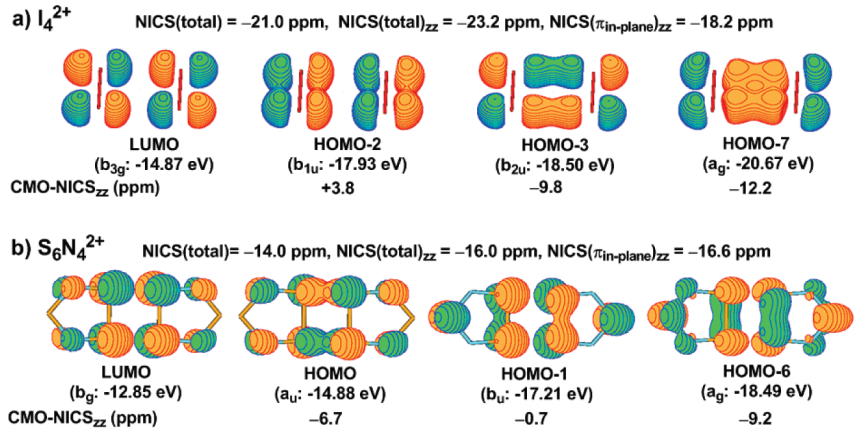

Figure 2. Selected molecular orbitals of I_4^{2+} (D_{2h}) and $(S_3N_2)_2^{2+}$ (C_{2h}) that are involved in the 4c-6e through-space π-conjugations. The eigenvalues of these MOs are at MPW1PW91/SDB-cc-pVTZ for I_4^{2+} and at B3LYP/6-311+G(3df) for $(S_3N_2)_2^{2+}$. CMO NICS values were computed at PW91PW91 with the SDB-cc-pVTZ basis set for I_4^{2+} and the 6-31G* basis set for $(S_3N_2)_2^{2+}$.

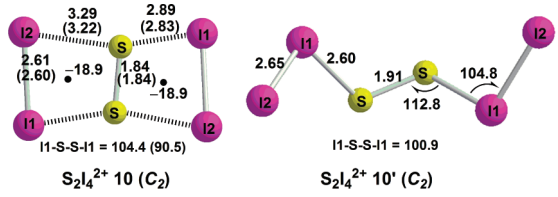

Figure 3. MPW1PW91 geometries (bond lengths in Å and angles in degrees) and GIAO-NICS values (in ppm) of $S_2I_4^{2+}$ **10** and its acyclic isomer **10′**. Experimental data (in parentheses) are from ref 21a.

normal S−S single bond), with a bond order of 2.2−2.4, estimated with X-ray crystallographic and vibrational spectroscopic data.[21] This C_2-symmetric dication (Figure 3) consists of two I_2 species weakly bound to a central S_2 moiety with two different I···S distances of 2.83 and 3.22 Å (experimental data). Since the dihedral angle I1−S−S−I1 is 90.5°, the two S_2I_2 planes are nearly perpendicular to each other. The MPW1PW91-optimized geometry of free $S_2I_4^{2+}$ **10** is in line with X-ray diffraction data and previous theoretical prediction.[21b] The energy of this "bicyclic" structure is predicted to be 2.1 kcal/mol lower than that of its acyclic isomer **10′**, despite the latter's two explicit 2.60 Å S−I bonds.

Scheme 4 illustrates the orbital interactions between the neutral S_2 molecule and I_2^+ cations in either the *xz*- and *yz*-plane of $S_2I_4^{2+}$ **10**. Passmore et al.[21] proposed that the high S−S bond order in $S_2I_4^{2+}$ was due to a neutral S_2 molecule (with a bond order of 2) interacting with two I_2^+ cations in two mutually perpendicular planes via the unpaired electrons (at the π^*-orbitals of the S_2 molecule) donating into the π^* orbitals of each I_2^+. Note that the 4c-6e $\pi^*-\pi^*$ bonding between the neutral S_2 moiety and an I_2^+ cation in each S_2I_2 plane of $S_2I_4^{2+}$ **10** is analogous to the 4c-6e $\pi^*-\pi^*$ bonding in I_4^{2+} discussed in subsection 3.1. Hence, the $I_2^+-S_2$ interactions in $S_2I_4^{2+}$ **10** can be understood better as arising from 4c-6e through-space in-plane π-conjugation. The $S_2I_4^{2+}$ dication possesses two sets of 4c-6e through-space in-plane π-conjugations, each located in a S_2I_2 plane. Alternatively, the $S_2I_4^{2+}$ dication can be regarded as a S_2^{2+} dication (with bond order 3) interacting with two I_2 molecules, each of which donates electrons from the doubly occupied π-orbitals to the corresponding empty π^*-orbitals of the central S_2^{2+} species. The unusual bonding between the S_2 and I_2 subunits in $S_2I_4^{2+}$ also can be understood in terms of VB theory. As shown in Scheme 5, the resonance of two VB structures, **10A** ($I_2^+S_2I_2^+$) and **10B** ($I_2S_2^{2+}I_2$), accounts for the observed structure of $S_2I_4^{2+}$. NBO analysis[49] on the MPW1PW91 Kohn−Sham wave functions of $S_2I_4^{2+}$ reveals the natural charges of +0.46 on the S_2 subunit and +0.77 on each I_2 subunit, as well as a S−S bond order of 2.25, conforming the electron delocalization in **10** and suggesting that the VB structure **10A** contributes dominantly to the ground-state structure of **10**.

Since $S_2I_4^{2+}$ has two separate 4c-6e through-space in-plane homoconjugation sets, both of its S_2I_2 planes should display in-plane PTS-like aromaticity. Indeed, the GIAO-NICS value at the center of each S_2I_2 plane, −18.9 ppm (Figure 3), confirms the dual PTS-like aromaticity of $S_2I_4^{2+}$ **10**. The aromatic through-space homoconjugation results in diamagnetic susceptibility exaltation; a MSE value of −33.5 ppm·cgs is derived for $S_2I_4^{2+}$ **10**, based on −147.6 ppm·cgs computed for polycyclic $S_2I_4^{2+}$ **10** and the much smaller value (χ = −114.1 ppm·cgs) for its acyclic chain isomer **10′** (Figure 3).

Note that $S_2I_4^{2+}$ **10** differs significantly from the isovalent $Se_2I_4^{2+}$ and P_2I_4[50] in structure. Figure 4 depicts the MPW1PW91-optimized geometries of $Se_2I_4^{2+}$ and P_2I_4. For P_2I_4, the computed structure agrees well with the experimentally determined structure.[50] The two PI_2 subunits in P_2I_4 are connected by a normal P−P single bond. In contrast, $Se_2I_4^{2+}$ has no classic covalent bond between its two eclipsed SeI_2^+ subunits; the inter-subunit interaction can be attributed to the aromatic 6c-10e through-space homoconjugation.[18] No conventional covalent bond exists between the S_2 and I_2^+ subunits of $S_2I_4^{2+}$ **10**; instead, they are united by two 4c-6e through-space in-plane homoconjugation sets.

3.3. Bishomoaromatic Inorganic Ion: Te_6^{2+}. Te_6^{2+} **11** was characterized as a C_{2v}-symmetric, boat-shaped six-membered ring in the inorganic salts, $[Te_6^{2+}][MOCl_4^-]_2$ (M = W, Nb).[23] The MPW1PW91-optimized geometry for free boat-shaped C_{2v} Te_6^{2+} (**11a**, Figure 5) agrees well with the experimental data. Notably, this dication contains "weak transannular interactions between the central two pairs of Te atoms",[47] with the transannular Te2−Te6/Te3−Te5 distances ranging between 3.21 and 3.38 Å. By assuming that the positive charge of this dication is mainly localized within the central two pairs of Te atoms,[51]

(49) Carpenter, J. E.; Weinhold, F. *J. Mol. Struct. (Theochem)* **1988**, *169*, 41.
(50) (a) Zak, Z.; Cernik, M. *Acta Crystallogr. C* **1996**, *52*, 290. (b) Leung, Y. C.; Waser, J. *J. Phys. Chem.* **1956**, *60*, 539.
(51) NBO analysis on the MPW1PW91-computed Kohn−Sham wavefunctions of **11a** revealed that the natural charges of the central four Te atoms sum up to +1.4.

Scheme 4. Orbital Interactions between the Neutral S_2 Molecule and I_2^+ Cations in the (a) *xz*-Plane and (b) *yz*-Plane of $S_2I_4^{2+}$

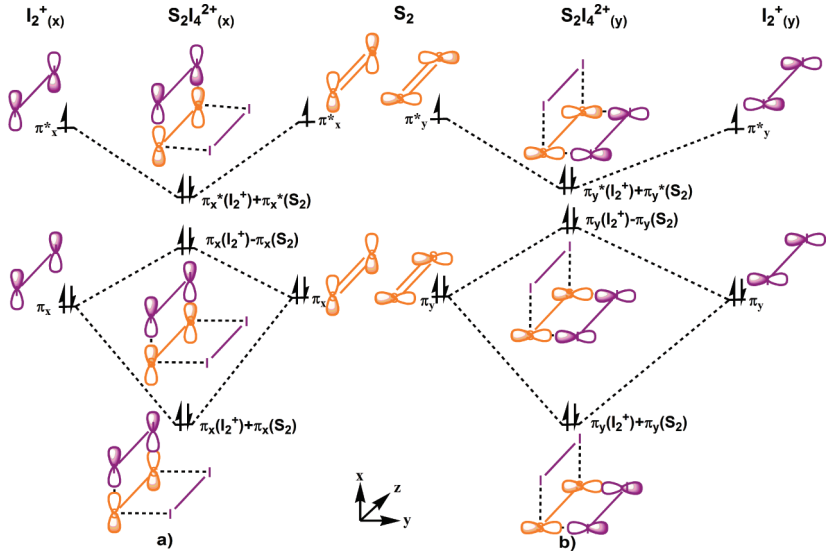

Scheme 5. Two VB Structures of $S_2I_4^{2+}$

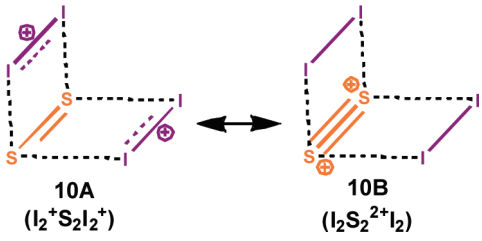

a "4c-6e $\pi^*-\pi^*$ bond" between the central Te_2 (Te2−Te3) and Te_2 (Te5−Te6) subunits[47] was previously proposed to account for such unusual transannular interactions, like the 4c-6e $\pi^*-\pi^*$ bond in I_4^{2+}. As with I_4^{2+}, the interaction arising from such 4c-6e $\pi^*-\pi^*$ bond should be better regarded as 4c-6e through-space homoconjugation (cf. Scheme 3b), which conforms to the

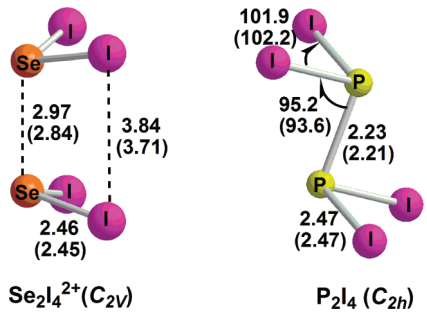

Figure 4. MPW1PW91-predicted geometry (bond lengths in Å and angles in degree) of $Se_2I_4^{2+}$ (ref 18) and P_2I_4. Experimental data are given in parentheses.

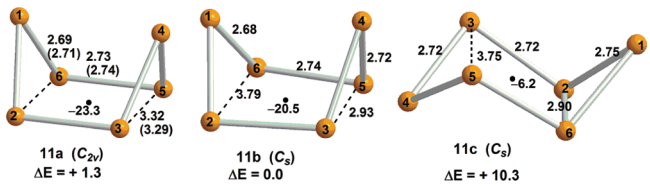

Figure 5. Optimized geometries (bond length in Å), symmetries, relative energies (ΔE in kcal/mol), and GIAO-NICS values (in ppm) of Te_6^{2+} isomers **11a**−**11c** from MPW1PW91 computations. The experimental data for the key geometric parameters (ref 23) are given in parentheses.

(4*N*+2) rule of aromaticity. The computed NICS value of −23.3 ppm for Te_6^{2+} **11a** (Figure 5) indicates that the 4c-6e through-space homoconjugation gives rise to a diatropic (aromatic) ring current in the central Te_4 (Te2−Te3···Te5−Te6) plane.

However, the C_{2v}-symmetric **11a** is not a minimum at the MPW1PW91/SDB-cc-pVTZ level; it is a transition state connecting two equivalent C_s-symmetric, boat-shaped Te_6^{2+} minima **11b** (Figure 5). The very small energy difference (1.3 kcal/mol) between **11a** and **11b** suggests that the transannular bond is highly flexible in nature. Isomer **11b** also is homoaromatic, with a NICS value of −20.5 ppm; shortening of the Te3−Te5 or Te2−Te6 distance does not change the nature of the transannular bonding remarkably. Selected molecular orbitals of Te_6^{2+} **11b** shown in Figure 6 account for the 4c-6e through-space homoconjugation between the two pairs of central Te atoms. The two apical Te atoms (Te1 and Te4) have minor contributions (cf. HOMO−5 and HOMO−8) to such a through-space conjugation. Thus, the boat-shaped Te_6^{2+} **11b** could be bishomoaromatic in nature.

In addition to the boat-shaped isomers **11a** and **11b**, we found a chair-shaped Te_6^{2+} isomer **11c** (Figure 5), which is 10.3 kcal/mol higher in energy than **11b** and is weakly aromatic, with a

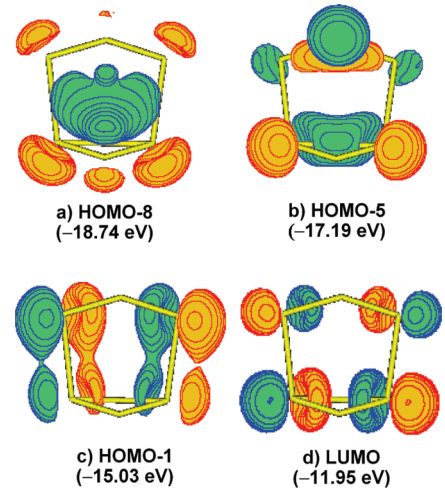

Figure 6. Molecular orbitals (at MPW1PW91/SDB-cc-pVTZ) of the boat-shaped Te_6^{2+} **11b** involving the 4c-6e through-space homoconjugation.

Scheme 6. Different Alignments of $5p_\pi$-Orbitals Involved in the Transannular Bonding in the Boat and Chair Isomers of Te_6^{2+}

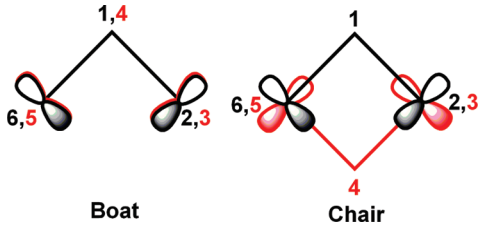

very small NICS value of −6.2 ppm. The higher energy and weaker aromaticity can be attributed to the much poorer transannular bonding and π-conjugation in **11c**. As shown in Scheme 6, the $5p_\pi$-orbitals involved in the transannular bonding in the boat isomer **11b** (or **11a**) are parallel, and this improves the orbital overlap and the through-space conjugation, whereas in the chair isomer the $5p_\pi$-orbitals at Te2/Te5 and Te3/Te6 are orthogonal, with much poorer $5p_\pi$(Te2)−$5p_\pi$(Te3)/$5p_\pi$(Te5)−$5p_\pi$(Te6) orbital overlap and, hence, much weaker π-electron delocalization.

3.4. Spherically Homoaromatic Inorganic Ions: Te_6^{4+} (D_{3h}) as Well as the Hypothetical S_6^{4+} and Se_6^{4+}. The trigonal prismatic tetracation Te_6^{4+}(D_{3h}) **12** in the inorganic salts, $[Te_6^{4+}][AsF_6^-]_4 \cdot 2SO_2$ and $[Te_6^{4+}][AsF_6^-]_4 \cdot 2AsF_3$,[25] consists of two eclipsed triangular Te_3^{2+} monomers (Figure 7). Previous DFT computations predicted an elongated trigonal prism as the ground-state structure of free Te_6^{4+}.[52] The optimized geometry of free Te_6^{4+}(D_{3h}) **12** at MPW1PW91/SDB-cc-pVTZ is in line with the experimental structure (Figure 7). The distance between the two triangular Te_3^{2+} planes (experimental ∼3.12 Å vs theoretical 3.34 Å) is longer than a normal single Te−Te bond (∼2.76 Å) but much shorter than the sum of two van de Waals radii of Te (∼4.3 Å). This geometric feature implies substantial through-space intermonomer bonding interaction to compensate for the remarkable electrostatic repulsion between two dicationic monomers. The through-space bonding interaction in Te_6^{4+} **12** has been rationalized, using MO theory, as "a $\pi^*-\pi^*$ six centre four electron (6c-4e) bond of the two unpaired electrons residing in the π^* orbital of Te_3^{2+} moieties",[47,53] i.e., the degenerate e′ orbitals depicted in Scheme 7. In addition, the interaction of the fully occupied π-orbitals of two Te_3^{2+} subunits results in the a_1' and a_2'' MOs of Te_6^{4+}, the former being bonding and the latter antibonding (for details, see Figure S3 in Supporting Information). As a whole, such through-space bonding interaction in Te_6^{4+} involves a total of eight electrons pertaining to the $5p_\pi$ orbitals of the six Te atoms.

This point can be understood more conveniently in terms of VB theory. As shown in Scheme 8, three VB structures (**12A**−**12C**), each containing two intermonomer σ-bonds and

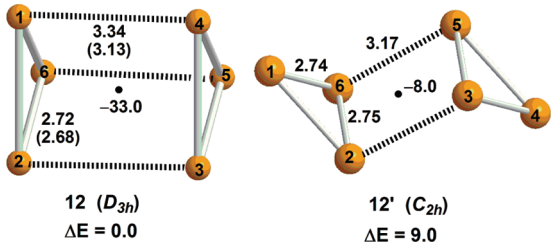

Figure 7. Optimized geometries (bond length in Å), symmetries, relative energies (ΔE in kcal/mol), and GIAO-NICS values (in ppm) of Te_6^{4+} isomers **12** and **12′** from MPW1PW91 calculations. The experimental data for the key geometric parameters (ref 25) are given in parentheses.

Scheme 7. Schematic Representations of Molecular Orbitals of Te_6^{4+} **12** Derived from the π- and π^*-Orbitals of the Te_3^{2+} Monomers, and the Computed CMO-NICS Values of Each Molecular Orbital

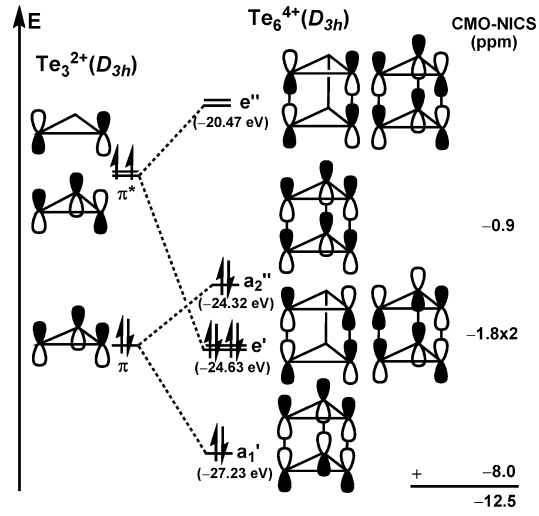

Scheme 8. Resonance of three VB structures of Te_6^{4+} **12** accounting for the 6c−8e through-space conjugation

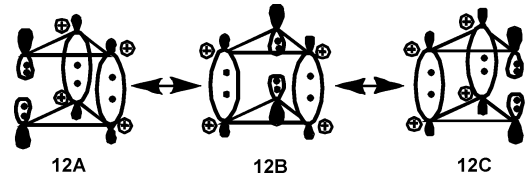

two nonbonding lone pairs, can be drawn to account for the intermonomer bonding that involves the $5p_\pi$ orbitals of the six Te atoms. The resonance among these equivalent VB structures gives rise to electron delocalization, namely, *six-center, eight-electron (6c-8e) through-space conjugation*. Such 6c-8e through-space homoconjugation is three-dimensional and, meanwhile, conforms to the $2(N+1)^2$ rule of spherical aromaticity.[12]

The spherical aromaticity of Te_6^{4+} **12** arising from the 3D 6c-8e through-space conjugation can also be rationalized by grouping its π-MOs according to spherical harmonics.[9a] On the basis of their symmetries and eigenvalues, the four occupied π-MOs (Scheme 7) of the D_{3h}-symmetric Te_6^{4+} can be classified into two groups of spherical harmonic MOs, i.e., the a_1' orbital of the S group ($L = 0$) and the e′ and a_2'' orbitals belonging to the P group ($L = 1$). Spherical aromaticity is thus attained by completely filling these spherical harmonic MOs ($L_{max} = 1$) with $2(L_{max}+1)^2 = 8$ electrons.[9a]

The spherical aromaticity of this tetracation is documented by its negative isotropic NICS value (−33.0 ppm at GIAO-MPW1PW91/SDB-cc-pVTZ, −31.4 ppm at GIAO-PW91PW91/SDB-cc-pVTZ) as well as the significant diatropic contribution (−12.5 ppm, Scheme 7) of the eight through-space-conjugated electrons to the total NICS. In addition, the σ-framework of each Te_3^{2+} monomer possesses aromatic σ-electron delocalization, analogous to the aromatic σ-electron conjugation in

(52) Lyne, P. D.; Mingos, D. M. P.; Ziegler, T. *J. Chem. Soc., Dalton Trans.* **1992**, 2743.
(53) Burford, N.; Passmore, J.; Sanders, J. C. P. *From Atoms to Polymers, Isoelectronic Analogies*; Liebman, J. F., Greenberg, A., Eds.; VCH: Weinheim, 1989; p 53, and references therein.

Table 1. MPW1PW91-Computed Key Atomic Distances (Å), NICS (ppm), and HOMO−LUMO Gap (E_g, eV) for D_{3h}-Symmetric X_6^{4+} (X = Te, Se, S)

	Te_6^{4+} **12**	Se_6^{4+} **13**	S_6^{4+} **14**
$R(XX)_S$[a]	2.72	2.34	2.06
$R(XX)_L$[b]	3.34	2.98	2.75
NICS[c]	−33.0	−39.1	−42.7
E_g	3.85	4.43	4.62

[a] Intramonomer X−X bond length. [b] Intermonomer X−X distance. [c] Computed at the cage center.

cyclopropane.[54] Owing to its spherical aromaticity, the cage-shaped Te_6^{4+} **12** has a large diamagnetic susceptibility (−195.7 ppm·cgs) and is 9.0 kcal/mol more stable than its chair-shaped C_{2h}-symmetric isomer **12′** (Figure 7). The latter is weakly aromatic, with a GIAO-predicted NICS (at the center of the Te2−Te3−Te5−Te6 tetragon) of −8.0 ppm as well as a much smaller diamagnetic susceptibility of −104.0 ppm·cgs (CSGT-predicted value).

Are the two experimentally unknown tetracations, Se_6^{4+} **13** and S_6^{4+} **14**,[55] the lighter homologues of Te_6^{4+} **12**, likely to be viable and to possess similar spherical homoaromaticity? The computed geometric parameters, NICS values, and HOMO−LUMO gaps of three X_6^{4+} (X = Te, Se, S) tetracations are listed in Table 1. All three X_6^{4+} (X = Te, Se, S) tetracations have similar D_{3h}-symmetric, trigonal prismatic structures consisting of two eclipsed trigonal X_3^{2+} monomers. Their intermonomer X−X distances are ∼0.65 Å longer than their intramonomer X−X bond lengths but much shorter than the sum of van der Waals radii of X. They do exhibit similar intermonomer through-space homoconjugation and spherical aromaticity. The predicted isotropic NICS(0) values are −42.7 ppm for S_6^{4+}, −39.1 ppm for Se_6^{4+}, and −33.0 ppm for Te_6^{4+}, suggesting that the through-space conjugation increases on going up the group. Along with the increase of spherical homoaromaticity, the HOMO−LUMO gap also increases from 3.85 eV for Te_6^{4+} to 4.62 eV for S_6^{4+}, implying higher kinetic stability and possible viability of the lighter tetracations, Se_6^{4+} **13** and S_6^{4+} **14**.

3.5. Neutral Bishomoaromatic Inorganic Compounds: 1,5-Diphosphadithiatetrazocines. Experimental realization of neutral bishomoaromatic organic systems is not trivial,[6e,56] although several model systems have been predicted theoretically.[57] However, the neutral 1,5-diphosphadithiatetrazocines, synthesized more than 20 years ago,[24] have not been recognized to be bishomoaromatic until now.

Scheme 9. 1,5-Diphoshadithiazocines **15a**−**15c** and the p_π Orbitals of the V-Shaped NSN Subunits

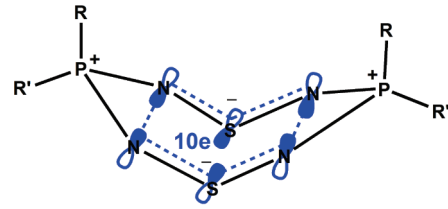

Table 2. B3LYP-Computed Key Atomic Distances[a] (Å), NICS[b] (ppm), $NICS_{zz}$[b] (ppm), Magnetic Susceptibility[c] (χ, ppm·cgs), and Magnetic Susceptibility Exaltation[d] (Λ, ppm·cgs) for the 1,5-Diphosphadithiatetrazocines PRR′$(NSN)_2$PRR′ Compounds **15a**−**15c** and the Energy Differences[e] (ΔE, kcal/mol) between **15a**−**15c** and Their Acyclic Isomers **16a**−**16c**

	15a R = Me R′ = Me	**15b** R = Ph R′ = Ph	**15c** R = Cl R′ = CCl_3
S−N	1.60(1.60)	1.59(1.59)	1.60(1.59)
P−N	1.62(1.63)	1.62(1.62)	1.60(1.61)
S···S	2.62(2.55)	2.63(2.53)	2.62(2.53)
N···N	2.67	2.68	2.67
NICS	−18.9	−16.9	−17.5
$NICS_{zz}$	−13.8	−14.7	−15.0
χ	−135.8	−242.6	−235.6
Λ	−22.7	−33.5	−35.6
ΔE	−52.0	−51.3	−45.5

[a] The experimental data extracted from ref 24 are given in parentheses. [b] NICS at the center of the $(NSN)_2$ portion. The z-axis is the C_2-axis of the C_{2v}-symmetirc molecules. [c] χ predicted by the CSGT method. [d] $\Lambda = \chi(\mathbf{15}) - \chi(\mathbf{16})$; **16** is the acyclic isomer of **15**. [e] $\Delta E = E(\mathbf{15}) - E(\mathbf{16})$.

Our B3LYP computations reproduced the geometries of 1,5-diphosphadithiatetrazocines PRR′$(NSN)_2$PRR′ **15a**−**15c** (Scheme 9 and Table 2). These structures display interesting transannular S···S interactions (S···S distances around 2.54 Å). All N atoms in these compounds are dicoordinated, with transannular N···N distances around 2.67 Å. The S−N bond lengths around 1.60 Å[24] are shorter than expected for a normal S−N single bond (∼1.77 Å), implying the presence of S−N π-bonding. The P−N bond length around the four-coordinated P atom is essentially similar to that of phosphazenes (e.g., $N_mP_mR_{2m}$, m = 3, 4; R = F, Cl), i.e., dominantly "ionic" P^+−N σ-bond with minor contribution from the negative hyperconjugation (the $\pi_N \rightarrow \sigma^*_{PR}$ interaction).[58] Therefore, each V-shaped $(NSN)^-$ subunit in **15** has a three-center, five-electron (3c-5e) π-bond consisting of the $p_\pi(N)$ and $p_\pi(S)$ atomic orbitals (Scheme 9), which is analogous to the 3c-5e π-bond of the V-shaped SeI_2^+ subunit in $Se_2I_4^{2+}$ (Scheme 3).[18] Figure 8 depicts the selected Kohn−Sham orbitals of **15a**, which illustrate the through-space head-to-head interaction of two 3c-5e π-bonds of $(NSN)^-$ subunits. Such 6c-10e through-space $\pi-\pi$ interaction is analogous to the bishomoaromatic 6c-10e through-space homoconjugation in S_8^{2+} and Se_8^{2+} cations[18] and results in bishomoaromaticity in **15a**−**15c**.

Alternatively, the 6c-10e through-space $\pi-\pi$ interaction in **15** can be represented by three VB structures **15A**−**15C** (Scheme 10) involving a transannular N−N or S−S σ-bond. The resonance of these VB structures results in the 6c-10e

(54) For original papers on σ-aromaticity, see: (a) Dewar, M. J. S. *Bull. Soc. Chim. Belg.* **1979**, *88*, 957. (b) Dewar, M. J. S.; McKee, M. L. *Pure Appl. Chem.* **1980**, *52*, 1431. (c) Dewar, M. J. S. *J. Am. Chem. Soc.* **1984**, *106*, 669. For a recent review, see ref 10, the section on σ-aromaticity and σ-antiaromaticity.

(55) A D_{3h}-symmetric structure of S_6^{4+} was predicted previously. See: Krossing, I.; Passmore, J. *Inorg. Chem.* **2004**, *43*, 1000.

(56) (a) Goren, A. C.; Hrovat, D. A.; Seefelder, M.; Quast, H.; Borden, W. T. *J. Am. Chem. Soc.* **2002**, *124*, 3469. (b) Quast, H.; Seefelder, M. *Angew. Chem., Int. Ed.* **1999**, *38*, 1064. (c) Quast, H.; Seefeder, M.; Becker, C.; Heubes, M.; Peters, E.-M.; Peters, K. *Eur. J. Org. Chem.* **1999**, 2763. (d) Jackman, L. M.; Fernandes, E.; Heubes, M.; Quast, H. *Eur. J. Org. Chem.* **1998**, 2209.

(57) (a) Wu, H.-S.; Jiao, H.; Wang, Z.-X.; Schleyer, P. v. R. *J. Am. Chem. Soc.* **2003**, *125*, 10524. (b) Brown, E. C.; Henze, D. K.; Borden, W. T. *J. Am. Chem. Soc.* **2002**, *124*, 14977. (c) Reiher, M.; Kirchner, B. *Angew. Chem., Int. Ed.* **2002**, *41*, 3429. (d) Hrovat, D. A.; Williams, R. V.; Goren, A. C.; Borden, W. T. *J. Comput. Chem.* **2001**, *22*, 1565. (e) Jiao, H.; Nagelkerke, R.; Kurtz, H. A.; Williams, R. V.; Borden, W. T.; Schleyer, P. v. R. *J. Am. Chem. Soc.* **1997**, *119*, 5921. (f) Jiao, H.; Schleyer, P. v. R. *Angew. Chem., Int. Ed. Engl.* **1993**, *32*, 1760.

(58) Chaplin, A. B.; Harrison, J. A.; Dyson, J. P. *Inorg. Chem.* **2005**, *44*, 8407.

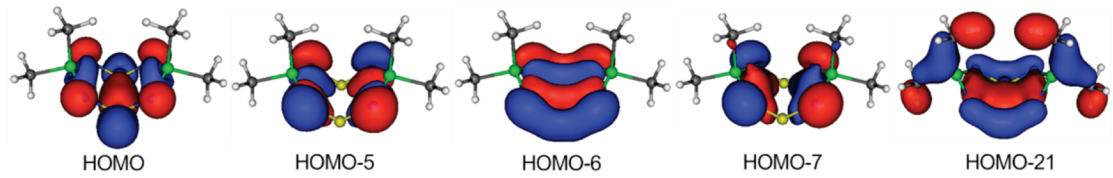

Figure 8. Selected molecular orbitals responsible for the through-space 6c-10e $\pi-\pi$ interaction in $P(CH_3)_2(NSN)_2P(CH_3)_2$.

Scheme 10. Three VB Structures Accounting for the 6c-10e Through-Space Homoconjugation between the p_π-Orbitals of the Two V-Shaped $(NSN)^-$ Subunits in 1,5-Diphoshadithiatetrazocines

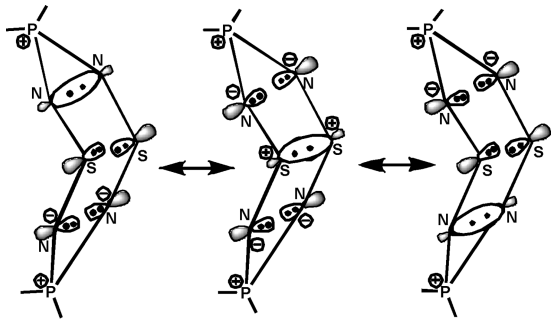

through-space homoconjugation, which conforms to the Hückel aromaticity rule. Accordingly, the 1,5-diphoshadithiazocines **15a**−**15c** should be bishomoaromatic. The 1,5-diphoshadithiazocines **15a**−**15c** are diamagnetic, with negative NICS values ranging from −16.9 to −18.9 ppm at the center of the $(NSN)_2$ moiety; in agreement, the corresponding $NICS_{zz}$ values range from −13.8 to −15.0 ppm (Table 2).

The bishomoaromaticity of the 1,5-diphoshadithiazocines **15a**−**15c** is further confirmed by their computed magnetic susceptibility exaltations, −22.7, −33.5, and −35.6 ppm·cgs, respectively (Table 2), in comparison with their nonaromatic acyclic isomers **16a**−**16c**. The energies also document the neutral bishomoaromaticity, as the 1,5-diphoshadithiazocines **15a**−**15c** are 52.0, 51.3, and 45.5 kcal/mol more stable than their nonaromatic acyclic isomers **16a**−**16c**, respectively.

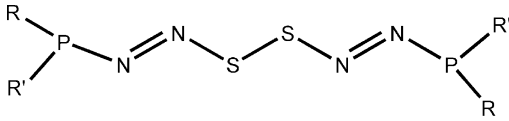

16a R=R'=Me 16c R=Cl, R'=CCl3
16b R=R'=Ph

Note that the bishomoaromatic 1,5-diphoshadithiazocines **15a**−**15c** have only modestly elongated transannular S···S distances (∼2.54 Å vs the 2.05 Å S−S single bond length in S_8), in contrast to the large increase in the transannular N···N separations (∼2.67 Å vs the 1.50 Å N−N single bond length). This implies that the VB contributor **15B** (Scheme 10) dominates the ground-state structure of 1,5-diphoshadithiazocines **15a**−**15c**. The importance of stronger transannular S···S interactions for the 6c-10e through-space homoconjugation between two $(NSN)^-$ subunits was demonstrated by considering two hypothetical barbaralane-like $[C_3H_4N_4X_2]^{2-}$ (X = S, O) dianions, **17** and **18** (Figure 9), which can have similar 6c-10e through-space homoconjugation (see Figure S4 in Supporting Information). The greater flexibility offered by the saturated C_3H_4 linkage allows stronger transannular N···N interactions. Indeed, the computed transannular N···N distances (around 2.44

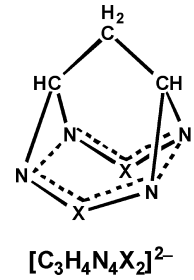

	17 (X=S)	18 (X=O)
X···X	2.84	3.09
N···N	2.44	2.44
X-N	1.61	1.39
N-X-N	114.2	124.6
NICS	−16.0	−9.4
$NICS_{ZZ}$	−10.7	−14.0

Figure 9. Barbaralane-like $[C_3H_4N_4X_2]^{2-}$ (X = S, O) anions, selected geometric parameters (in Å and degrees), and isotropic NICS(0) values (ppm) computed at GIAO-B3LYP/6-311+G(3df).

Scheme 11. Structures of Bridged 1,6-Y-[10]annulenes

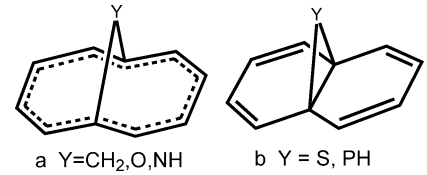

a Y=CH_2,O,NH b Y = S, PH

Å) in **17** and **18** are ∼0.23 Å shorter than those of 1,5-diphoshadithiazocines **15a**−**15c** and are even shorter than the homoconjugative ∼2.55 Å N···N distance in the bishomoaromatic bisdiazene−teroxide dication.[59] In contrast, the transannular S···S distance in $[C_3H_4N_4S_2]^{2-}$ **17** is ∼0.2 Å longer than that in **15a**−**15c**, whereas the transannular O···O distance (3.09 Å) in $[C_3H_4N_4O_2]^{2-}$ **18** is too large to allow any direct O−O bonding interaction. Despite the much weaker transannular X···X interaction in $[C_3H_4N_4X_2]^{2-}$ (X = S, O), the GIAO-B3LYP NICS values for **17** (−16.0 ppm) and **18** (−9.4 ppm) show these systems to be bishomoaromatic as well.

We have shown that the 6c-10e through-space homoconjugative interactions between two $(NXN)^-$ subunits (X = S, O) in compounds **15a**−**15c**, **17**, and **18** are aromatic, though differing in the strength of transannular X···X interaction between the central atoms. If a transannular X−X single bond were formed, homoaromaticity would not be maintained. This situation is similar to the effects of the perturbing transannular interactions in bridged 1,6-Y-[10]annulenes. Previous theoretical investigations[60] illustrated that the bridged 1,6-Y-[10]annulenes (Y = CH_2, O, NH) prefer delocalized structures (see Scheme 11a) and are aromatic, whereas their Y = PH and S counterparts favor bisnorcaradiene structures with a transannular C−C bond (see Scheme 11b) and are nonaromatic. B3LYP/6-311++G(3df) optimizations of initial geometries of **15a**−**15c**, **17**, and **18** having imposed X−X single bond distances between the two central atoms (X = S, O) led to minima with opened transannular X···X separations (Table 2 and Figure 9). This shows

(59) Exner, K.; Prinzbach, H.; Gescheidt, G.; Grossman, B.; Heinze, J. *J. Am. Chem. Soc.* **1999**, *121*, 1964.
(60) (a) Mealli, C.; Ienco, A.; Hoyt, E. B., Jr.; Zoellner, R. W. *Chem.—Eur. J.* **1997**, *3*, 958. (b) Jiao, H.; Hommes, N. J. R. v. E.; Schleyer, P. v. R. *Org. Lett.* **2002**, *4*, 2393.

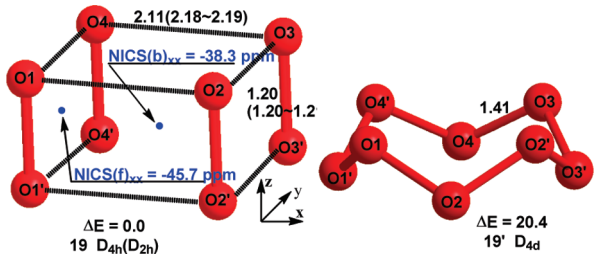

Figure 10. B3LYP/6-311++G(3df)-optimized geometry (key bond lengths in Å) and relative energy (ΔE, kcal/mol) of $(O_2)_4$ **19** (D_{4h}) and its D_{4d}-symmetric isomer **19′**. Experimental data are given in parentheses. NICS(b)$_{xx}$ and NICS(f)$_{xx}$ denote the *xx* tensors of NICS at the cage center and at the face center, respectively. For the $(O_2)_4$ **19** (D_{4h}), NICS(b)$_{xx}$ = NICS(b)$_{yy}$.

that the X···X interactions are not strong enough to maintain transannular X−X single bonds. Nevertheless, the 6c-10e through-space homoconjugative interactions in **15a**−**15c**, **17**, and **18** are analogous to the homoconjugation in $Se_2I_4^{2+}$ (Figure 4),[18] which has a strong Se···Se interaction between the two SeI_2^+ subunits. In contrast, the isovalent P_2I_4 (Figure 4) has a P−P single bond between the two PI_2 subunits and is nonaromatic.

3.6. $(O_2)_4$ Unit of ε-Phase Solid Oxygen: Quadruple PTS-like Homoaromaticity. The free O_2 molecule has a paramagnetic triplet ground state ($^3\Sigma_g^-$). However, recent experiments disclosed that high-pressure ε-phase solid oxygen[61] consists of diamagnetic $(O_2)_4$ **19** structural units.[22] Such an $(O_2)_4$ unit (Figure 10) was found to be rhomboid-shaped and D_{2h}-symmetric, with two characteristic bond angles of 84° (O4−O1−O2 and O4−O3−O2) and 96° (O3−O2−O1 and O1−O4−O3) as well as two characteristic interatomic distances of 1.20−1.21 Å (O−O bond length in the O_2 subunits) and 2.18−2.19 Å (O−O distance between O_2 subunits),[22] implying an unconventional bonding interaction between O_2 subunits. Quantum chemical calculations at both the MP2/6-31+G(d) and the B3LYP/6-311++G(3df) levels of theory predict that isolated $(O_2)_4$ **19** has a cuboid structure with D_{4h} symmetry, differing slightly from the D_{2h}-symmetric rhomboid structure observed in ε-O_2 solid. The B3LYP-optimized geometry of **19** is depicted in Figure 10. It should be noted that a classic VB structure of O_8 is the crown-shaped structure **19′** of D_{4d} symmetry, analogous to the well-characterized structure of its sulfur congener, S_8.[62] However, this structure is 20.4 kcal/mol higher in energy than $(O_2)_4$ **19** at the B3LYP/6-311++G(3df) level. At the same level of theory, $(O_2)_4$ **19** is unstable by ∼66 kcal/mol with respect to four $O_2(^3\Sigma_g^-)$ molecules. This explains why diamagnetic $(O_2)_4$ **19** can only be observed under high pressure.

The interactions between O_2 subunits have been ascribed in terms of MO theory to $2\pi^*-2\pi^*$ MO interactions.[63] That is, each O_2 subunit has two singly occupied $2\pi^*$ orbitals; the combination of eight $2\pi^*$ MOs of four O_2 subunits gives rise

(61) For a recent review on solid oxygen, see Freyman, Y. A.; Jodl, H. J. *Phys. Rep.* **2004**, *401*, 1.
(62) (a) Kim, K. S.; Jang, J. H.; Kim, S.; Mhin, B.-J.; Schaefer, H. F. *J. Chem. Phys.* **1990**, *92*, 1887. (b) Zhao, M.; Gimarc, B. M. *J. Phys. Chem.* **1993**, *97*, 4023. (c) Politzer, P.; Lane, P. *Int. J. Quantum Chem.* **2000**, *77*, 336.
(63) Steudel, R.; Wong, M. W. *Angew. Chem., Int. Ed.* **2007**, *46*, 1768. These authors claimed that a rhomboid structure with D_{2h} symmetry is a local $(O_2)_4$ minimum at the G3X(MP2) level of theory, whereas a cuboid structure with D_{4h} symmetry is a local minimum at the DFT level of theory. However, G3X(MP2) theory actually adopts geometry optimized at the hybrid density functional B3LYP/6-31G(2df,p) level of theory.

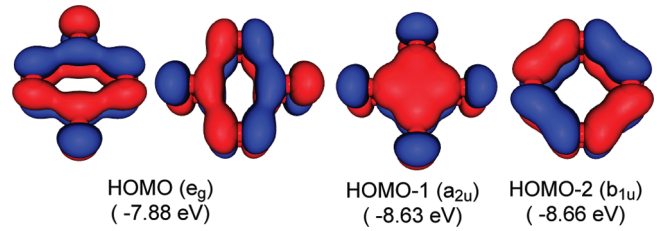

Figure 11. Selected Kohn−Sham orbitals (isodensity value ∼0.04) of $(O_2)_4$ **19** consisting of the $2\pi^*$ MOs of four O_2 ($^3\Sigma_g^-$) molecules. Eigenvalues and symmetries of these MOs are given in parentheses.

Scheme 12

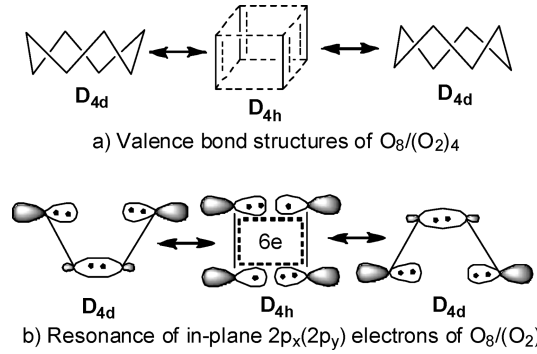

to four doubly occupied MOs of $(O_2)_4$ **19**, as depicted in Figure 11. Our alternative interpretation of the unconventional O_2-O_2 interactions within $(O_2)_4$ **19** is based on VB theory. As shown in Scheme 12a, $(O_2)_4$ **19** can be regarded as an intermediate VB state connecting two equivalent classic VB structures **19′** (D_{4d}). In $(O_2)_4$ **19**, each O_2 subunit has two sets of p_π atomic orbitals, $2p_x$ and $2p_y$ orbitals of O atoms. Thus, in an O_2-O_2 plane, four in-plane p_x (or p_y) atomic orbitals of four oxygen atoms can form 4c-6e in-plane through-space conjugation (Scheme 12b), as a result of the resonance between two equivalent localized VB structures **19′** (D_{4d}). Such 4c-6e in-plane conjugation is analogous to the 4c-6e in-plane conjugation within I_4^{2+} described above and is PTS-like aromatic according to the Hückel aromaticity rule. Thus, $(O_2)_4$ **19** has quadruple aromatic 4c-6e in-plane conjugations, each pertaining to a local O_2-O_2 plane. The PTS-like aromaticity of such 4c-6e through-space conjugation is shown by the remarkably negative NICS$_{ii}$ (ii = xx for the O1−O1′−O4−O4′ and O2−O2′−O3−O3′ planes or ii = yy for the O1−O1′−O2−O2′ and O4−O4′−O3−O3′ planes) value at the center of an O_2-O_2 plane (NICS(f)$_{ii}$ = −45.7 ppm, see Figure 10). In addition, the NICS(b)$_{ii}$ (ii = xx or yy) value of −38.3 ppm at the cage center is smaller in absolute value than NICS(f)$_{ii}$, as a result of in-plane conjugation.

4. Concluding Remarks

We extended the aromatic through-space homoconjugation concept, well-established in organic chemistry, to inorganic systems having through-space $\pi^*-\pi^*$ bonding(s) between two weakly interacting subunits. Depending on their geometries and the number of electrons involved in their through-space conjugations, the aromaticity exhibited by the inorganic species can be differentiated into several types, including *PTS-like aromaticity* of I_4^{2+}, $S_6N_4^{2+}$, $S_2I_4^{2+}$, and $(O_2)_4$ (in ε-O_2 solid), *bishomoaromaticity* of Te_6^{2+} and 1,5-diphosha-dithiatetrazocines, and *spherical aromaticity* of X_6^{4+} (X = Te, Se, S). The aromaticity of these inorganic ions and

compounds is documented by their highly negative NICS values. The $S_2I_4^{2+}$ dication, $(O_2)_4$ (in ε-O_2 solid), and the neutral 1,5-diphoshadithiatetrazocines are of particular interest. The $S_2I_4^{2+}$ dication is disclosed to have two orthogonal sets of 4c-6e through-space in-plane conjugations in its two S_2I_2 planes, which account for its unusually high S−S bond order and result in dual PTS-like aromaticity. The cuboid $(O_2)_4$ has quadruple PTS-like aromaticity arising from 4c-6e through-space in-plane conjugation pertaining to its O_2-O_2 planes. The long-known 1,5-diphoshadithiatetrazocines are found to be neutral bishomoaromatic species. This finding should encourage further experimental searches for neutral bishomoaromatic organic compounds.[56,57]

Acknowledgment. This work was sponsored in China by NSFC (Grants No. 20425312, 20673088, 20721001, 20423002), the 973 Program (Grant No. 2007CB815307), and Xiamen University through a Minjiang Professorship, and in USA by National Science Foundation Grant CHE-0716718 and the Institute for Functional Nanomaterials (NSF Grant 0701525).

Supporting Information Available: Figures S1−S4, Cartesian coordinates, total energies, electronic states, and number of imaginary frequency predicted for the ions and compounds studied, and complete ref 45a. This material is available free of charge via the Internet at http://pubs.acs.org.

JA9029285